A Reinvestigation of Excitation Source of the CS_2+(A^2Π_u- X^2Π_g) Emission in the Ar Afterglow: Both Ar^+ and Ar_2^+ Ions Can Be Excitation Sources Giving Significantly Different Spectral Features

TSUJI, Masaharu
Institute for Materials Chemistry and Engineering, and Research and Education Center of Green Technology, Kyushu University

ENDOH, Minoru
Department of Molecular Science and Technology, Interdisciplinary Graduate School of Engineering, Kyushu University : Graduate Student

FUNATSU, Tsuyoshi
Department of Molecular Science and Technology, Interdisciplinary Graduate School of Engineering, Kyushu University : Graduate Student

NAKAMURA, Masafumi
Department of Molecular Science and Technology, Interdisciplinary Graduate School of Engineering, Kyushu University : Graduate Student

他

https://doi.org/10.15017/4795519

出版情報：九州大学大学院総合理工学報告. 44 (1), pp.1-11, 2022-09. 九州大学大学院総合理工学府
バージョン：
権利関係：

九州大学大学院総合理工学府報告
第 44 巻 第 1 号 1-11 頁 令和 4 年 9 月

Engineering Sciences Reports, Kyushu University
Vol. 44, No. 1, pp. 1-11, SEP, 2022

A Reinvestigation of Excitation Source of the $CS_2^+(\tilde{A}^2\Pi_u - \tilde{X}^2\Pi_g)$ Emission in the Ar Afterglow: Both Ar^+ and Ar_2^+ Ions Can Be Excitation Sources Giving Significantly Different Spectral Features

Masaharu TSUJI[*1,2†] Minoru ENDOH[*3] Tsuyoshi FUNATSU[*3] Masafumi NAKAMURA[*3] Keiko UTO[*1] Jun-Ichiro HAYASHI[*1] and Takeshi TSUJI[*4]
[†]E-mail of corresponding author: tsuji@cm.kyushu-u.ac.jp

(Received March 18, 2022, accepted April 18, 2022)

In 1984, we have reported that $CS_2^+(\tilde{A}^2\Pi_u - \tilde{X}^2\Pi_g)$ visible emission in an Ar flowing afterglow arises from the $Ar_2^+ + CS_2$ charge-transfer (CT) reaction at thermal energy.[1)] In 1986, Upshulte et al.[2)] claimed that Ar^+ not Ar_2^+ is the responsible excitation source of the $CS_2^+(\tilde{A}-\tilde{X})$ emission in their flow-tube study. Although more than 36 years have passed since these two-original flowing-afterglow studies, no definite conclusion has been obtained on the exact excitation source of the $CS_2^+(\tilde{A}-\tilde{X})$ emission in the Ar afterglow. To confirm whether Ar_2^+ and/or Ar^+ really contributes to the $CS_2^+(\tilde{A}-\tilde{X})$ emission, additional experiments were carried out in this flowing-afterglow study. Results show that the conclusion of Upshulte et al.[2)] is wrong and that both Ar^+ and Ar_2^+ can be excitation sources of $CS_2^+(\tilde{A}-\tilde{X})$ emissions, though spectral features are quite different between the two reactions. The $Ar_2^+ + CS_2$ reaction gives discrete $CS_2^+(\tilde{A}-\tilde{X})$ emission bands from low vibrational levels, whereas the $Ar^+ + CS_2$ reaction dominantly provides continuous $CS_2^+(\tilde{A}-\tilde{X})$ emission from high rovibrational levels. The higher vibrational excitation of the $CS_2^+(\tilde{A})$ state than that expected from vertical Franck-Condon (FC) like ionization was confirmed by the re-examination of reported ion cyclotron resonance (ICR) data.

Key words: *$CS_2^+(\tilde{A}-\tilde{X})$ emission, Flowing afterglow, Ar^+ ion, Ar_2^+ ion, Charge-transfer reaction, Franck-Condon factor, Energy-resonant requirement, Kinetic energy ICR*

1. Introduction

In 1984, we have reported an optical spectroscopic study on the Ar afterglow reaction of CS_2.[1)] A strong visible $CS_2^+(\tilde{A}^2\Pi_u - \tilde{X}^2\Pi_g)$ emission from low vibrational levels were observed. Possible excitation sources were Ar^+, Ar_2^+, and Ar^{+*}(metastable ion) because this emission disappeared by trapping ionic species using ion-collector grids placed between the discharge section and the reaction zone. To determine the responsible excitation source, the dependence of emission intensity of $CS_2^+(\tilde{A}-\tilde{X})$ on the Ar pressure was compared with that of $OCS^+(\tilde{A}-\tilde{X})$ emission from the $Ar^+ + OCS$ reaction[3)] and CH(A–X) emission from the $Ar^{+*} + CH_3CN$ reaction.[4)] The $CS_2^+(\tilde{A}-\tilde{X})$ emission increased its intensity with increasing the Ar pressure from 0.3 to 4 Torr (1 Torr = 133.32 Pa), although the $OCS^+(\tilde{A}-\tilde{X})$ and CH(A–X) emissions gave peaks at 0.5 and 0.4 Torr and rapidly decreased their intensities with increasing the Ar pressure to 1 Torr. Based upon these facts, we concluded that the excitation source of $CS_2^+(\tilde{A}-\tilde{X})$ was not Ar^+ or Ar^{+*} but Ar_2^+.

After our flowing-afterglow study, two follow-up studies have been carried out by famous groups in the fields of gas phase ion chemistry in the world: Castleman's group in Penn State[2)] and Bowers's group in UC Santa Barbara.[5)] Upshulte et al.[2)] carried out a flowing-afterglow optical spectroscopic study on the $CS_2^+(\tilde{A}-\tilde{X})$ emission in 1986. Based on the disappearance of this emission by ion trapping and variations of emission intensity of the $CS_2^+(\tilde{A}-\tilde{X})$ emission as a function of Ar pressure, flow velocity of discharge flow, or the glow discharge voltage, they concluded that the excitation source was

*1 Institute for Materials Chemistry and Engineering, and Research and Education Center of Green Technology
*2 Department of Molecular Science and Technology
*3 Department of Molecular Science and Technology, Graduate Student
*4 Department of Materials Science, Shimane University

the thermal-energy $Ar^+ + CS_2$ CT reaction and not the $Ar_2^+ + CS_2$ CT reaction, we suggested.[1] Although they did not notice, there was a significant difference in spectral features of $CS_2^+(\tilde{A}\text{–}\tilde{X})$ emission between their and our spectra. Their $CS_2^+(\tilde{A}\text{–}\tilde{X})$ emission was much broader than our spectrum due to an appearance of strong continuous background band.

After above two works, Rincon et al.[5] investigated the $Ar^+ + CS_2$ CT reaction at thermal and near thermal energies in 1988 by using both tandem ICR spectroscopy and kinetic energy ICR. At thermal energy, the rate constant was measured as 2.9×10^{-10} cm^3 $molecule^{-1}$ s^{-1}, and branching ratios of S^+ and CS_2^+ were determined to be 97 and 3%, respectively.

$$Ar^+ + CS_2 \rightarrow S^+ + CS + Ar \quad (97\%) \quad (1a)$$
$$\rightarrow CS_2^+ + Ar \quad (3\%) \quad (1b)$$

Kinetic energy studies revealed that the CS_2^+ product is 90% formed in the $\tilde{A}^2\Pi_u$ state with a near Franck-Condon (FC) vibrational state distribution and 10% in the $\tilde{X}^2\Pi_g$ state.

$$Ar^+ + CS_2 \rightarrow CS_2^+(\tilde{A}^2\Pi_u) + Ar \quad (90\%) \quad (2a)$$
$$\rightarrow CS_2^+(\tilde{X}^2\Pi_g) + Ar \quad (10\%) \quad (2b)$$

The S^+ product in process (1a) is formed exclusively in the ground $S^+(^4S)$ state with the maximum kinetic energy allowed by energy and momentum conservation. These results imply that the $Ar^+ + CS_2$ CT reaction takes place via a long-range electron jump since no momentum transfer occurs in most part. On the other hand, the formation of minor $CS_2^+(\tilde{A}^2\Pi_u)$ state proceeds through short-range intimate collision accompanying with substantial momentum transfer. They reported that it is still possible that Ar_2^+ is the source of the $CS_2^+(\tilde{A}\text{–}\tilde{X})$ emission and that this reaction preferentially populates low vibrational states of $\tilde{A}^2\Pi_u$. However, this suggestion contradicted the previous conclusion of Upshulte et al.[2]

Although it takes more than 34 years after these three-pioneering works on the CT reactions of Ar^+ and Ar_2^+ with CS_2 leading to $CS_2^+(\tilde{A}\text{–}\tilde{X})$ emission,[1,2,5] no definite conclusion has been obtained until now on the exact excitation source of $CS_2^+(\tilde{A})$ in the Ar flowing afterglow. The objective of this work is to determine whether $Ar^+ + CS_2$ and/or $Ar_2^+ + CS_2$ CT reaction really participate in the formation of $CS_2^+(\tilde{A}\text{–}\tilde{X})$ emission based on new additional experiments in the flowing afterglow. In the previous two flowing-afterglow experiments,[1,2] only Ar afterglow was used for the study of ion-molecule reactions of CS_2. A disadvantage of the Ar afterglow experiment is that both Ar^+ and Ar_2^+ can contribute to the $CS_2^+(\tilde{A}\text{–}\tilde{X})$ emission, which makes difficult to assign its exact excitation source. In the present study, the contribution of the $Ar^+ + CS_2$ CT reaction is examined by using the He afterglow where only Ar^+ monomer ion is generated by the $He(2^3S) + Ar$ Penning ionization. In this case, the contribution of the $Ar_2^+ + CS_2$ CT reaction is completely excluded. Then, the contribution of the $Ar_2^+ + CS_2$ reaction is examined by comparing the $CS_2^+(\tilde{A}\text{–}\tilde{X})$ emission spectrum obtained from the $Ar^+ + CS_2$ CT reaction in the He afterglow with that in the Ar afterglow at various Ar pressures. Active ionic species produced in the Ar afterglow are also monitored using mass spectrometry to examine ionic species in the flow tube. The rovibrational distribution of $CS_2^+(\tilde{A})$ by the thermal-energy $Ar^+ + CS_2$ reaction is discussed based on re-examination of kinetic energy ICR data reported by Rincon et al.[5]

2. Experimental

Figures 1(a) and 1(b) show Ar afterglow and He afterglow apparatuses used in this study. The Ar afterglow apparatus was the same as that used previously.[1] The Ar afterglow apparatus was used for the study of the $Ar^+ + CS_2$ and $Ar_2^+ + CS_2$ reactions, whereas the He afterglow apparatus was employed for the study of the $Ar^+ + CS_2$ CT reaction. In the Ar afterglow experiment, CS_2 gas was added from the first entry port in Fig. 1(a). Typical partial pressures of Ar (purity 99.9999%) and CS_2 were 0.5–1.5 Torr and 3 mTorr, respectively.

In the He afterglow, high purity He gas (99.995%) was passed through a flow tube evacuated by a 10 000 L min^{-1} mechanical booster pump. Such He active species as $He(2^3S)$, He^+, and He_2^+ were generated by a 2.45 GHz microwave discharge at a He pressure of 0.60–0.70 Torr. The relative concentrations of $He(2^3S)$, He^+, and He_2^+ at 0.65 Torr have been estimated to be 1.0:1.5:0.05, respectively.[6] On addition of Ar gas from the first entry port and a target CS_2 gas from the second entry port, a conical reaction flame was observed around the second entry port. Typical partial pressures of He, Ar, and CS_2 were 600–700, 40, and 3 mTorr, respectively.

Green flames were observed in the Ar or He

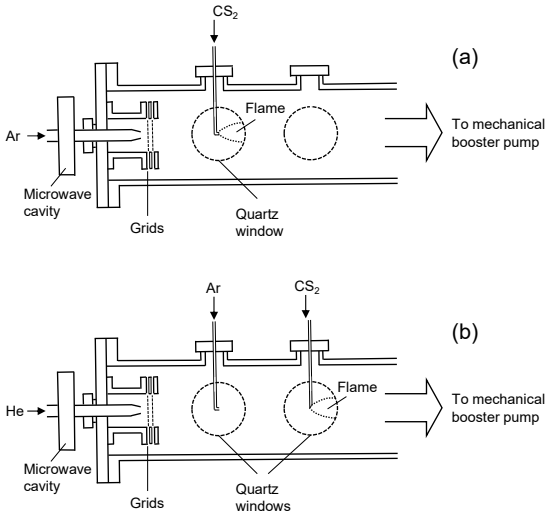

Fig. 1. (a) Ar flowing-afterglow and (b) He flowing-afterglow apparatuses used for the thermal-energy CT reactions of Ar^+ and Ar_2^+ with CS_2.

afterglow through a quartz window. Emission spectra in the 450–600 nm region were measured with a Jarrell Ash 1 m monochromator equipped with an HTV R585 photomultiplier.

Mass spectra of Ar ionic species in the Ar afterglow were measured using a similar apparatus reported previously.[7)]

3. Results and Discussion

3.1 Active species formed by microwave discharge in Ar and He afterglows

By microwave discharge of Ar gas, $Ar(^3P_{0,2})$, Ar^+, Ar^{+M}, and Ar_2^+ can be formed as active species. From mass spectroscopic measurements, we confirmed that Ar^+ and Ar_2^+ ions are present in our conditions as ionic active species. The $[Ar_2^+]/[Ar^+]$ ratio increases with increasing the Ar gas pressure because Ar_2^+ ions are formed by the termolecular reaction.

$$Ar^+ + 2Ar \xrightarrow{k_3} Ar_2^+ + Ar \qquad (3)$$

$k_3 = (2.7 \pm 0.3) \times 10^{-31}$ cm^6 molecule^{-2} s^{-1}.[8)]

By microwave discharge of He gas, neutral $He(2^3S)$ atoms with an excitation energy of 19.82 eV, and He^+ and He_2^+ ions with recombination energies of 24.59 eV and 18.3–20.3 eV, respectively, are generated as active species. When He^+ and He_2^+ ions were removed from the discharge flow using the ion-collector grids and the Ar gas was injected from the first entry port in Fig. 1(b), only neutral $He(2^3S)$ atoms can go downstream along the flow tube and arrive at the reaction zone. Then, the following Penning ionization and associative ionization occur around the first entry port with a rate of 7.5×10^{-11} cm^3 molecule^{-1} s^{-1}.[9)]

$$He(2^3S) + Ar \rightarrow Ar^+(^2P_{1/2,3/2}) + He + e^- \quad (87\%) \qquad (4a)$$

$$\rightarrow HeAr^+ + e^- \quad (13\%) \qquad (4b)$$

The branching ratio of (4a) and (4b) was measured to be 0.87:0.13, respectively.[10-12)] Reaction (4a) provides $Ar^+(^2P_{1/2,3/2})$ ions and Penning electrons. The recombination energies of $Ar^+(^2P_{1/2})$ and $Ar^+(^2P_{3/2})$ are 15.94 and 15.76 eV, respectively. The initial $[Ar^+(^2P_{1/2})]/[Ar^+(^2P_{3/2})]$ ratio in the $He(2^3S)$ + Ar Penning ionization has been measured to be about 0.5 by using Penning ionization electron spectroscopy.[13)] The $[Ar^+(^2P_{1/2})]/[Ar^+(^2P_{3/2})]$ ratio in the reaction zone was estimated by observing ArF* excimer emission resulting from the $Ar^+(^2P_{1/2,3/2})$ + SF_6^- ionic recombination reaction.[14)] On the basis of our optical spectroscopic studies on the spin-orbit state selective formation of rare gas monofluoride excimers,[14,15)] the ArF(B-X,C-A) excimers are selectively formed from the $Ar^+(^2P_{3/2})$ + SF_6^- reaction, while the ArF(D-X) excimer preferentially results from the $Ar^+(^2P_{1/2})$ + SF_6^- reaction. Therefore, the intensity ratio of ArF(D-X)/ArF(B-X,C-A) reflects the $[Ar^+(^2P_{1/2})]/[Ar^+(^2P_{3/2})]$ ratio. The only ArF(B-X,C-A) excimers were observed by addition of a small amount of SF_6 into the reaction zone, when Ar^+ was formed both by the $He(2^3S)$ + Ar Penning ionization and by a microwave discharge of Ar. This suggests that the upper $Ar^+(^2P_{1/2})$ spin-orbit component relaxes to the lower $Ar^+(^2P_{3/2})$ one by superelastic collisions with electrons under our conditions.[16)]

$$Ar^+(^2P_{1/2}) + e^- \rightarrow Ar^+(^2P_{3/2}) + e^- \qquad (5)$$

$HeAr^+(X^2\Sigma^+)$ produced from reaction (4b) has a small dissociation energy of D_0 = 207 cm^{-1}.[17)] This binding energy is smaller than the kinetic energy of He buffer gas at 300 K (39 mV = 313 cm^{-1}). Therefore, $HeAr^+(X^2\Sigma^+)$ heterodimer cluster ions dissociate into He + Ar^+ by collision with He buffer gas.[18)]

$$HeAr^+(X^2\Sigma^+) + He \rightarrow Ar^+ + 2He \qquad (6)$$

The most important point in the He afterglow experiment is that Ar partial pressure (40 mTorr) is too low to generate Ar_2^+. The only presence of Ar^+ and the absence of Ar_2^+ and $HeAr^+$ in the present He afterglow experiments were confirmed by the mass spectroscopic measurement of product ions.

3.2 $CS_2^+(\tilde{A}^2\Pi_u$–$\tilde{X}^2\Pi_g)$ emissions resulting from $Ar_2^+ + CS_2$ CT reaction in the Ar afterglow and $Ar^+ + CS_2$ CT reaction in the He afterglow

Figure 2(a) shows a typical emission spectrum of the $CS_2^+(\tilde{A}\,^2\Pi_u - \tilde{X}\,^2\Pi_g)$ transition obtained in the Ar afterglow at a high Ar gas pressure of 1.3 Torr. This emission was similar to that observed at a higher Ar pressure of 2.6 Torr in our previous study.[1)] Besides strong $CS_2^+(\tilde{A}–\tilde{X})$ emissions from the ground vibrational $0^0 = (0,0,0)$ levels, weak $CS_2^+(\tilde{A}–\tilde{X})$ emissions from such low vibrational levels as $1^1 = (1,0,0)$ and $2^2 = (0,2,0)$ are identified in both two Ω =1/2 and 3/2 spin-orbit components. Besides the principal (0,0,0)–(v_1″,0,0) bands for v_1″= 0–2 and (0,0,0)–(v_1″–1,2,0) Fermi resonant bands for v_1″ = 1 and 2, weak (1,0,0)–(0,0,0), (0,2,0)–(0,0,0), and (0,2,0)–(0,2,0) bands from the excited v_1' = 1 and v_2' = 2 levels are identified.[1,19)] We concluded that this $CS_2^+(\tilde{A}–\tilde{X})$ emission arises from the $Ar_2^+ + CS_2$ CT reaction at thermal energy in our previous study.[1)]

Figure 2(b) shows a typical emission spectrum obtained from the $Ar^+ + CS_2$ CT reaction using the He afterglow apparatus shown in Fig. 1(b). It should be noted that spectral features are quite different from those of the $Ar_2^+ + CS_2$ reaction (Fig. 2(a)). In Fig. 2(b), a strong continuous band is observed, as reported by Upschlte et al. under low spectral resolution.[2)] In addition, some weak discrete bands, which are ascribed to $CS_2^+(\tilde{A}–\tilde{X})$ emissions from the (0,0,0), (1,0,0), and (0,2,0) levels, are found over strong continuous bands. The relative intensities of the $CS_2^+(\tilde{A}–\tilde{X})$ emissions from the excited (1,0,0) + (0,2,0) levels to those from the ground (0,0,0) vibrational levels in Fig. 2(b) are stronger than those in Fig. 1(a) by a factor of about 3. This result shows that $CS_2^+(\tilde{A}–\tilde{X})$ emission in Fig. 2(b) is more vibrationally excited than that in Fig. 2(a).

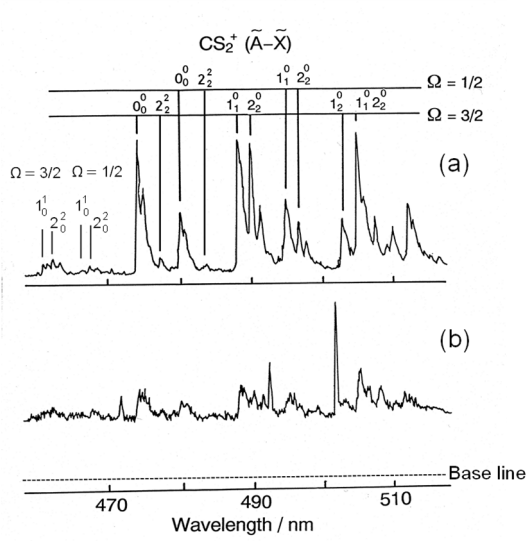

Fig. 2. $CS_2^+(\tilde{A}\,^2\Pi_u - \tilde{X}\,^2\Pi_g)$ emissions resulting from (a) the thermal-energy Ar_2^+ CS_2 CT reaction in the Ar afterglow and (b) the thermal-energy $Ar^+ + CS_2$ CT reaction in the He afterglow.

Similar unidentified continuous emissions have been observed from CS_2 in the UV-visible region as background emission of the discrete $CS_2^+(\tilde{A}–\tilde{X})$ bands under fast electron-impact excitation,[20,21)] $He(2^3S)$, $He(2^1S)$, and $Ne(^3P_{0,2})$ Penning ionization,[22-25)] and $CO^+ + CS_2$ CT reaction at thermal energy.[21)] The most outstanding features of the continuous emission in the $Ar^+ + CS_2$ reaction are that its relative intensity to the discrete $CS_2^+(\tilde{A}–\tilde{X})$ bands is much higher than those observed in other ionization processes described above.[20-25)]

The continuous emission with nearly constant intensity appears in the whole wavelength range of 460–515 nm including the shorter wavelength region of the 0_0^0 origin bands of Ω = 3/2 and 1/2 components at 474 and 480 nm, respectively. The observation of strong continuous emission below the 0_0^0 bands indicates that vibrationally excited states of $CS_2^+(\tilde{A})$ are formed in the $Ar^+ + CS_2$ CT reaction. Although Upschlte et al.[2)] assigned to this continuous emission to $CS_2^+(\tilde{A}–\tilde{X})$ emission from high vibrational levels, they did not discuss exact reason why the $CS_2^+(\tilde{A}–\tilde{X})$ emission from high vibrational levels gives such a broad emission.

Figure 3 shows potential energy curves of CS_2 and $CS_2^+(\tilde{X},\tilde{A},\tilde{B})$ and recombination energies of Ar^+ and Ar_2^+. The internuclear distances of the $CS_2(X)$, $CS_2^+(\tilde{X})$, and $CS_2^+(\tilde{A})$ states are 1.5545, 1.5542, and 1.615 Å, respectively.[19,26,27)] Although the internuclear distances of the $CS_2(X)$ and $CS_2^+(\tilde{X})$ states are nearly the same, that of the $CS_2^+(\tilde{A})$ state is larger than that of the $CS_2(X)$ state by 0.06 Å. Therefore, Franck-Condon factors (FCFs) for $CS_2(X) \rightarrow CS_2^+(\tilde{A})$ ionization obtained by HeI

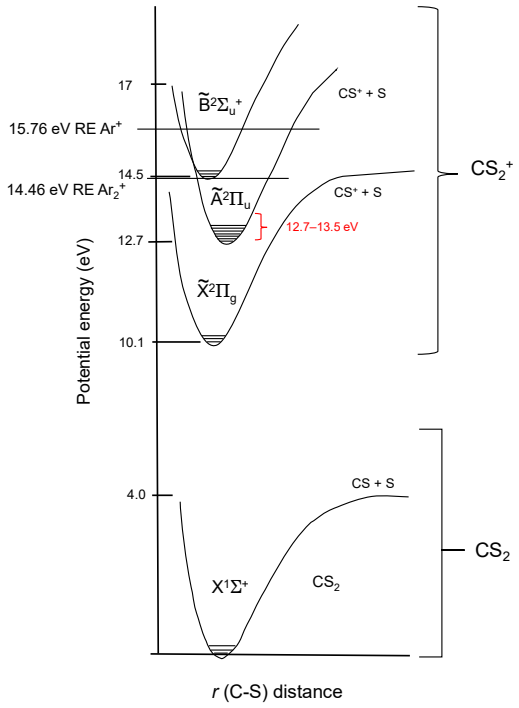

Fig. 3. Potential energy curves of CS_2 and CS_2^+ and recombination energies of Ar^+ and Ar_2^+(adiabatic value).

photoelectron spectrum (PES) have a broad distribution in the range of $CS_2^+(\tilde{A}:(0,0,0)$ – $(7,0,0))$ levels with a broad peak at v_1'=1–3: $(0,0,0) - (7,0,0) = 0.10 : 0.20 : 0.24 : 0.19 : 0.13 : 0.09 : 0.05 : 0.02$.[28] Although $CS_2^+(\tilde{A}–\tilde{X})$ emissions from $CS_2^+(\tilde{A}: v_1'$=0–7) are expected to be observed on the basis of FCFs for ionization given above, only $CS_2^+(\tilde{A}–\tilde{X})$ emissions from v_1'=0–3 or v_1'=0–4 and their Fermi-resonance levels were observed in vacuum ultraviolet (VUV) photoionization (λ = 92.3 nm),[29] fast electron-impact ionization,[30] and $He(2^3S)$ Penning ionization.[23] Under VUV photoionization where ionization proceeds through vertical FC-like ionization, dominant $CS_2^+(\tilde{A}–\tilde{X})$ emissions occur from v_1'=0–2 and those from v_1' = 3 and 4 are weaker than expected from FCFs. Wu et al.[29] attributed the absence of emissions from v_1' = 5 and 6 to small FCFs for the $CS_2^+(\tilde{A}–\tilde{X})$ transition.

If an excess energy released in the thermal-energy CT reaction is not favorably converted to translational energies of products, near-resonant internal-energy states will be formed dominantly. Although the $CS_2^+(\tilde{A}–\tilde{X})$ emission from v_1' > 4 level has not been observed, high vibrationally excited states with small FCFs for ionization will be formed in the $Ar^+ + CS_2$ CT reaction because energy-resonance requirement may take part in the reaction.

High vibrational states of $CS_2^+(\tilde{A})$ has been studied by Liu et al.[31] using high resolution pulsed field ionization-photoelectron (PFI-PE) spectroscopy. $CS_2^+(\tilde{A})$ peaks from (0,0,0) to (6,0,0) and (5,2,0) levels have been identified in the 12.69–13.13 eV region. In the energy region above 13.13 eV, the intensity of PFI-PE bands decreases significantly. Their calculations indicated that most of the PFI-PE bands in the higher energy region are strongly mixed due to anharmonic and Fermi resonances and polyads interactions so that the assignment of the vibrational quantum numbers is not possible. Thus, it is expected emissions from such high vibrationally excited states as $v_1' > 6$ consist of many complicated energy levels. Thus, if emission occurs from high vibrational levels, complicated emissions providing continuous emission will occur. The formation of complicated high vibrational levels due to Fermi resonance and Renner-Teller effects as observed by PFI-PE and laser induced fluorescence spectra[32,33] is one reason for the appearance of the continuous $CS_2^+(\tilde{A}–\tilde{X})$ emission from high vibrational levels.

In our previous optical spectroscopic studies on the Ar flowing-afterglow reaction of OCS,[34,35] $OCS^+(\tilde{A}\,^2\Pi_\Omega – \tilde{X}\,^2\Pi_\Omega$: Ω = 1/2, 3/2) emission resulting from the thermal-energy Ar^+ + OCS CT reaction was observed.

$$Ar^+(^2P_{3/2}) + OCS \rightarrow OCS^+(\tilde{A}:(0,0,0)) + Ar + 0.68\ eV. \quad (7)$$

The emission band widths of each $OCS^+(\tilde{A}–\tilde{X})$ emission were much broader than those obtained by $He(2^3S)$ and $Ne(^3P_{0,2})$ Penning ionization because of high rotational excitation of $OCS^+(\tilde{A})$. The fluorescence channel in the $OCS^+(\tilde{A}: 0,0,0)$ level was found to be open for rotationally excited levels up to $J \approx 170$ ($\approx$5500 cm^{-1}). The rotational distribution of $OCS^+(\tilde{A}^2\Pi_{3/2}:0,0,0)$ could be characterized by a Boltzmann temperature of 4300±500 K, indicating that 55±7% of the excess energy is deposited into the rotation of $OCS^+(\tilde{A})$. Since the excess energy of the $Ar^+ + CS_2 \rightarrow CS_2^+(\tilde{A}: 0,0,0) + Ar$ CT reaction, 3.1 eV, is much higher than that in the $Ar^+(^2P_{3/2}) + OCS \rightarrow OCS^+(\tilde{A}:(0,0,0)) + Ar$ CT reaction, 0.68 eV, similar or much higher rotational excitation is expected for many vibrational $CS_2^+(\tilde{A})$ states formed in the $Ar^+ + CS_2$ CT reaction. A high rotational excitation of $CS_2^+(\tilde{A})$ will be the other reason for the appearance of continuous band in the $CS_2^+(\tilde{A}–\tilde{X})$ emission from the $Ar^+ + CS_2$

CT reaction.

We concluded that strong unresolved background band arises from heavy overlapping of many emissions from high vibrational and rotational excited states of $CS_2^+(\tilde{A})$. They are major product channels in the $Ar^+ + CS_2$ CT reaction leading to the $CS_2^+(\tilde{A})$ state.

$$Ar^+ + CS_2 \rightarrow CS_2^+(\tilde{A}\text{: high vibrational levels: } v_1' > 4) + Ar \quad \text{(major product)} \qquad (8a)$$

Weak discrete bands are attributed to $CS_2^+(\tilde{A}-\tilde{X})$ emission from such low vibrational states as (0,0,0), (1,0,0), and (0,2,0). They are minor product channels in the $Ar^+ + CS_2$ CT reaction.

$$Ar^+ + CS_2 \rightarrow CS_2^+(\tilde{A}\text{: low vibrational levels: } v_1' = 0,1 \text{ and } v_2'' = 2) + Ar \quad \text{(minor product)} \qquad (8b)$$

Based on our previous study,[24] collisional relaxation from high vibrational levels of $CS_2^+(\tilde{A})$ to low vibrational ones occurs in the flowing afterglow. It is therefore reasonable to assume that not only direct formation but also collisional relaxation from high rovibrational levels to low rovibrational levels participates in the formation of low vibrational levels of $CS_2^+(\tilde{A})$.

It should be noted that our conclusion that highly rovibrationally excited states are dominant product states in the $Ar^+ + CS_2$ CT reaction is inconsistent with the ICR study by Rincon et al.[5] They predicted that the vibrational distribution of $CS_2^+(\tilde{A})$ is essentially FC-like one on the basis of kinetic energy ICR data of CS_2^+ ions. If the CT reaction occurs by a rapid electron jump at large internuclear separation, the transfer process is expected to be governed primarily by FCFs for vertical ionization. It has been known that $CS_2^+(\tilde{A}-\tilde{X})$ emissions observed by VUV photoionization and He(2^3S) Penning ionization of CS_2 proceed through FC-type vertical ionization,[23,29] so that $CS_2^+(\tilde{A}-\tilde{X})$ emissions from $v_1' = 0$–4 and 0–3 were observed, respectively. If $CS_2^+(\tilde{A}-\tilde{X})$ emission observed from the thermal-energy $Ar^+ + CS_2$ CT reaction proceeds also through FC-type vertical ionization, as predicted by Rincon et al.,[5] its spectral features should be similar to those observed by VUV photoionization and He(2^3S) Penning ionization of CS_2.[23,29] However, the observed spectral features of $CS_2^+(\tilde{A}-\tilde{X})$ emission from the $Ar^+ + CS_2$ CT reaction are significantly different from those by VUV photoionization and He(2^3S) Penning ionization of CS_2, where strong continuous emission was not observed. This finding also supports our conclusion that vibrational distribution of $CS_2^+(\tilde{A})$ in the thermal-energy $Ar^+ + CS_2$ reaction is non-FC-type one.

3.3 A re-examination of ICR data of Rincon et al.[5] for the $Ar^+ + CS_2 \rightarrow CS_2^+(\tilde{A}^2\Pi_u) + Ar$ CT reaction

In order to obtain information on the reason for the discrepancy between the present optical study and ICR measurements, ICR data reported by Rincon et al.[5] was re-examined. Figure 4(a) shows plot of the percentage of CS_2^+ ions trapped versus the square of the trapping voltage for the thermal-energy $Ar^+(^2P_{3/2}) + CS_2$ CT reaction leading to CS_2^+ parent ions. In general, ion kinetic energies can be determined in the ICR experiments by measuring the dependence of the fraction of the ions trapped on the trapped voltage.[5,36] When the electrostatic trapping well employed in the ICR is sufficiently deep, all of the ions are trapped in the ICR cell. However, as the well depth is decreased, kinetically excited ions will escape from the trap. For a positive singly charged ion, plots of the fraction of the ions trapped, f (%), versus the square root of the trapping potential, $(V_T)^{1/2}$, are expected to give two distinct linear regions described by

$$f = 100; \qquad V_T \geq E_T \qquad (9a)$$

$$f = (V_T / E_T)^{1/2} \times 100; \quad V_T < E_T \qquad (9b)$$

where E_T is the kinetic energy of the ions. For a reaction in which the products have only a single value of E_T, a plot of f versus $V_T^{1/2}$ is constant at $f = 100$ until $V_T = E_T$, at which point a break occurs and then linearly decreases to zero with decreasing $V_T^{1/2}$ to zero. The kinetic energy of the ions can be determined from the break between these two linear regions. In a real reaction system, a distribution of translational energies would be observed due to the vibrational and rotational distributions in the products. Consequently, instead of a sharp break, curvature will occur around the break point.

If the kinetic energy of CS_2^+ ion has a constant value, f should increase linearly until $V_T = E_T$ and then it keeps 100% at higher trapping voltage. Although f linearly increases from zero to $V_T^{1/2} = 0.87\ V^{1/2}$, it increases

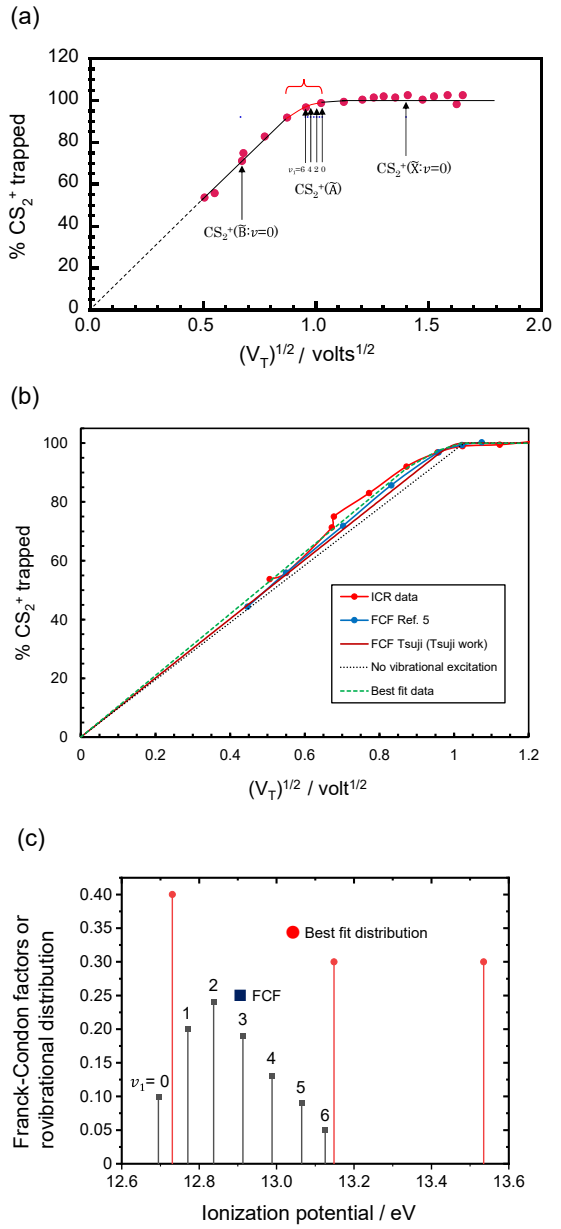

Fig. 4. (a) and (b) Plots of the percentage of CS_2^+ ions trapped versus the square root of the trapping voltage for the $Ar^+(^2P_{3/2})$ + CS_2 reaction to yield CS_2^+ product ions. ICR data of Ref. 5 are plotted as filled red circles. The threshold energies for the formation of the $\tilde{X}$, $\tilde{A}(v_1'=0–6)$, and $\tilde{B}$ states of CS_2^+ are shown in (a). The arrows in (a) are bracketing the non-linear part of the curve, thus indicating the approximate position and width of the kinetic energy distribution. In (b), observed $\%CS_2^+$ ions trapped versus $V_T^{1/2}$ is compared with those expected from FC-type vertical ionization (Ref. 5 and this work), no vibrational and rotational excitation, and best fit distribution. (c) detailed values of FCFs and best fit distribution used in (b).

nonlinearly from 0.87 $V^{1/2}$ to 1.02 $V^{1/2}$, and then it becomes nearly constant above 1.02 $V^{1/2}$, as shown in Fig. 4(a). This indicates that the kinetic energy of CS_2^+ ions is not constant, but it has a distribution in the $V_T^{1/2}$ = 0.87–1.02 $V^{1/2}$ range. Momentum conservation requires the corresponding minimum and maximum total kinetic energy release to be $TKE_{min} = E_T(CS_2^+) \times [(39.95 + 76.14)/39.95] = 2.2$ eV and $TKE_{max} = 3.0$ eV in the $CS_2^+ + Ar$ products. The ionization energies for CS_2^+, $IP(CS_2^+)$, at $V_T^{1/2}$ = 1.021, 0.958, and 0.875 $V^{1/2}$ states are estimated to be 12.73, 13.09, and 13.54 eV, respectively from the following relation.

$$IP(CS_2^+) = IP_0(CS_2^+) + IE(CS_2^+) = RE(Ar^+{:}15.76\ eV) - TKE(CS_2^+,Ar) \quad (10)$$

Here, $IP_0(CS_2^+)$, $IE(CS_2^+)$, RE, and $TKE(CS_2^+,Ar)$ are the ionization potential for $CS_2^+(\tilde{X})$, internal (electronic, vibrational, and rotational) energy of CS_2^+, the recombination energy of $Ar^+(^2P_{3/2})$, and the total kinetic energy released to CS_2^+ and Ar, respectively. Since the ionization energies for $CS_2^+(\tilde{A}: v_1' = 0–6)$ are 12.69–13.13 eV, besides these low energy states, higher energy $CS_2^+(\tilde{A}: v_1' > 6)$ states in the 13.13–13.54 eV region are expected to be formed in the $Ar^+(^2P_{3/2})$ + CS_2 CT reaction (Fig. 3). Such high energy states will be a source of continuous $CS_2^+(\tilde{A}–\tilde{X})$ emission.

In Fig. 4(b) are compared the observed f vs $V_T^{1/2}$ function in ICR experiments with those predicted from no vibrational and rotational excitation and from FC-type vertical ionization.[5] The f values obtained by assuming no vibrational and rotational excitation in the $CS_2^+(\tilde{A})$ state are smaller than the observed ones. This discrepancy suggests that $CS_2^+(\tilde{A})$ ions are vibrationally and/or rotationally excited. Then, we compared the observed f vs $V_T^{1/2}$ function with that expected from FC-type vertical ionization. Figure 4(b) shows two calculated data for FC-type ionization. One is reported data by Rincon et al.[5] and the other is our data obtained using reliable FCFs (Fig. 4(c)).[28] We obtained smaller f values than those reported by Rincon et al.[5] below $V_T^{1/2}$ = 1 $V^{1/2}$ (Fig. 4(b). We do not know the reason why the discrepancy is observed between our calculation and their results, because detailed FCFs for ionization they used were not reported. Rincon et al.[5] reported in Ref. 21 in their paper that "The vibrational distribution in the $\tilde{A}^2\Pi_u$ state formed by 2.1-eV photons is peaked at v_1'= 3 and covers a broad distribution from v_1' =

0 to $v_1' = 8$." Based on the standard PES data by Turner et al.[37] and Frost et al.,[28] this sentence should be revised as "The vibrational distribution in the $\tilde{A}^2\Pi_u$ state formed by 21.21-eV photons is peaked at $v_1' = 2$ and covers a broad distribution from $v_1' = 0$ to $v_1' = 7$." Thus, it seems that they did not use correct FCFs in their simulation. Anyway, there are still discrepancies between the observed f vs $V_T^{1/2}$ function and those calculated assuming FC-type ionization in the $V_T^{1/2}$ = 0.87–1.02 $V^{1/2}$ region, although Rincon et al.[5] reported that the vibrational distribution of the $\tilde{A}^2\Pi_u$ state is a near FC-type one. When the f vs $V_T^{1/2}$ function was simulated assuming various internal (vibrational and rotational) energy distributions in the $V_T^{1/2}$ = 0.87–1.02 $V^{1/2}$ region, a reasonable agreement between the observed and calculated functions was obtained using the following distribution (Fig. 4(c)): 40%, 30%, and 30% for IP(CS_2^+)=12.73, 13.09, and 13.54 eV, respectively. The internal energy distribution in the 13.1–13.5 eV region also supports the formation of high energy states above $CS_2^+(\tilde{A}: v_1' = 6)$, which will be responsible for the appearance of continuous $CS_2^+(\tilde{A}-\tilde{X})$ emission in the $Ar^+ + CS_2$ CT reaction.

Parent *et al.*[38] performed a systematic study on the thermal-energy CT reactions of Ar^+ with such triatomic molecules as H_2O, N_2O, and CO_2 using an ICR spectrometer. From the measured ion kinetic energy, the percentage of the excess energy, which is in internal energy (%TIE), was determined to be 48–70% for H_2O^+, 48–79% for N_2O^+, and 69–77% for CO_2^+. The mean %TIE values for H_2O^+, N_2O^+, and CO_2^+ are 59, 63.5, and 73%, respectively. On the basis of non-linear part in the kinetic energy distribution (Fig. 4(a)), we estimate the lower and upper limits of %TIE values for CS_2^+ to be TIE_{min} = 47% and TIE_{max} = 61%, respectively. The mean %TIE value is 54%. The internal energy distribution of CS_2 is narrower than those of H_2O, N_2O and CO_2, and its mean value is smaller than those of the three triatomic molecules.

3.4 $CS_2^+(\tilde{A}^2\Pi_u\text{-}\tilde{X}^2\Pi_g)$ emissions from thermal-energy $Ar_2^+ + CS_2$ and $Ar^+ + CS_2$ reactions in the Ar afterglow

In section 3.2, we can obtain $CS_2^+(\tilde{A}-\tilde{X})$ emission resulting solely from the $Ar^+ + CS_2$ CT reaction. Taking this result into consideration, we have re-investigated $CS_2^+(\tilde{A}-\tilde{X})$ emission in the Ar afterglow. In our previous work,[1] we measured $CS_2^+(\tilde{A}-\tilde{X})$ emission at a high Ar pressure of 2.6 Torr, where the concentration of Ar^+ is negligibly low. In this work, we measured $CS_2^+(\tilde{A}-\tilde{X})$ emissions at three typical Ar pressures of 1.3, 1.0, and 0.75 Torr. Results obtained are shown in Figs. 5(a)–5(c). It is noteworthy that significant changes in spectral features are observed. The spectrum at 1.3 Torr consists of only discrete bands without continuous background band, which agrees with our previous report.[1] With decreasing the Ar pressure from 1.3 to 1.0 Torr, the intensity of discrete bands decreases, and underground continuous band appears. With further decreasing the Ar gas pressure from 1.0 Torr to 0.75 Torr, the relative intensity of the discrete bands to the continuous band becomes small and the spectral features become similar to those observed in the $Ar^+ + CS_2$ reaction in the He afterglow (Fig. 2(b)). It is therefore reasonable to assume that major excitation source is Ar^+ monomer ion at the Ar pressure of 0.75 Torr. These results led us to conclude that $CS_2^+(\tilde{A}-\tilde{X})$ emission in the Ar afterglow consist of two components. One is only discrete bands without underground continuum band resulting from the $Ar_2^+ + CS_2$ CT reaction and the other is the weak discrete and strong underground continuum band resulting from

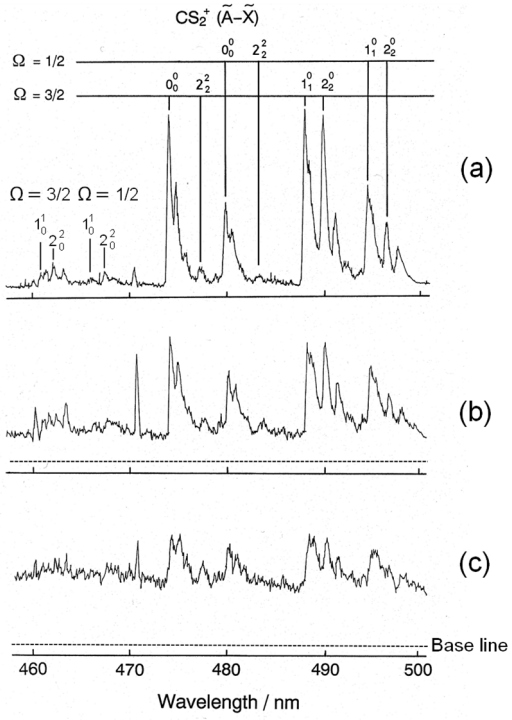

Fig. 5. $CS_2^+(\tilde{A}\ ^2\Pi_u - \tilde{X}\ ^2\Pi_g)$ emissions resulting from the Ar afterglow reaction of CS_2 at (a) 1.3 Torr, (b) 1.0 Torr, and (c) 0.75 Torr.

the $Ar^+ + CS_2$ CT reaction. The intensity ratio of resolved bands to underground continuous band of $CS_2^+(\tilde{A}-\tilde{X})$ emission depends on the $[Ar_2^+]/[Ar^+]$ ratio in each experimental condition. At high Ar pressures (e.g., 1.3 Torr), the former reaction is dominant, whereas the latter reaction occupies major part at low Ar pressures (e.g. 0.75 Torr). At intermediate Ar pressures (e.g. 1.0 Torr), both components are overlapped with each other.

On the basis of present results, the conclusion by Upshulte et al.[2] on the excitation source of $CS_2^+(\tilde{A}-\tilde{X})$ should be revised. They identified excitation source of $CS_2^+(\tilde{A}-\tilde{X})$ assuming that it is either Ar^+ or Ar_2^+ ion and the possibility of the contribution of both Ar^+ and Ar_2^+ ions was excluded. This made them wrong conclusion that only Ar^+ is the excitation source of $CS_2^+(\tilde{A}-\tilde{X})$.

We re-examined their reported $CS_2^+(\tilde{A}-\tilde{X})$ spectra observed at various experimental conditions.[2] With increasing the Ar pressure, decreasing the bulk flow velocity, and decreasing negative voltage, the intensity ratio of weak discrete bands to strong underground continuous bands increases (Figs. 3–5 in Ref. 2). These results can be explained by the increase in the $[Ar_2^+]/[Ar^+]$ ratio in their conditions. In our experiments, continuous background band nearly disappears at an Ar pressure above 1 Torr. However, in their experiments, weak continuous components remain even at high Ar pressures of 1.50 and 1.75 Torr. These results imply that the $[Ar^+]/[Ar_2^+]$ ratio in their experiments using glow discharge plasma was higher than that in our experiments using microwave discharge. Another reason for the appearance of background continuous bands in their experiments at high Ar pressures may be the observation region of emission spectra. Based on their flow-tube apparatus equipped with optical detection system (Fig. 2 in Ref. 2), they observed downstream emission spectra of the CS_2 gas inlet using an optical fiber. It seems that they did not detect emission directly around the CS_2 gas inlet, whose exit was facing in the opposite direction of the discharge flow. Therefore, they observed downstream emission from the CS_2 gas inlet. It has been known that the total reaction rate constant of the $Ar_2^+ + CS_2$ at thermal energy (8.8×10^{-10} cm^3 $molecule^{-1}$ s^{-1}) is 3.4 times larger than that of the $Ar^+ + CS_2$ reaction at thermal energy (2.9×10^{-10} cm^3 $molecule^{-1}$ s^{-1}).[5,39] It is therefore reasonable to assume that the $[Ar^+]/[Ar_2^+]$ ratio becomes large with increasing the distance of the observation region from the CS_2 gas inlet, leading to an enhancement of continuous $CS_2^+(\tilde{A}-\tilde{X})$ emission from the $Ar^+ + CS_2$ reaction.

The rate constant for the formation of $CS_2^+(\tilde{A})$ from the $Ar^+ + CS_2$ reaction is estimated to be 7.8×10^{-12} cm^3 $molecule^{-1}$ s^{-1} using a reported total reaction rate constant in a flow tube and the branching ratio for the formation of $CS_2^+(\tilde{A})$ (2.7%) obtained in the ICR experiment.[5] On the other hand, no information on the branching ratios of $CS_2^+(\tilde{A})$ and $CS_2^+(\tilde{X})$ have been obtained. Therefore, only the maximum value for the formation of $CS_2^+(\tilde{A})$, 8.8×10^{-10} cm^3 $molecule^{-1}$ s^{-1}, can be obtained assuming that the branching ratio of $CS_2^+(\tilde{A})$ is 100%. This value is larger than that in the $Ar^+ + CS_2$ reaction by two orders of magnitude.

Figure 6 shows potential energy curves of the ground $Ar_2^+(A^2\Sigma^+_{(1/2)u})$ and $Ar_2(X^1\Sigma^+_g)$ states. The adiabatic ionization potential of $Ar_2^+(A^2\Sigma^+_{(1/2)u}; v''=0)$ has been measured as 14.46 eV.[40,42] Although Ar_2^+ has a bound potential with a short equilibrium internuclear distance of 2.392 Å and a binding energy of 1.31 eV, $Ar_2(X^1\Sigma^+_g)$ potential has a weakly bound potential with a long equilibrium internuclear distance of 3.755 Å and a small binding energy of 0.01 eV.[40-42] Therefore, $Ar_2(X^1\Sigma^+_g)$ potential is repulsive in the FC width of $Ar_2^+(A^2\Sigma^+_{(1/2)u}; v''=0)$ as shown in Fig. 6. We have previously estimated the effective recombination energy of

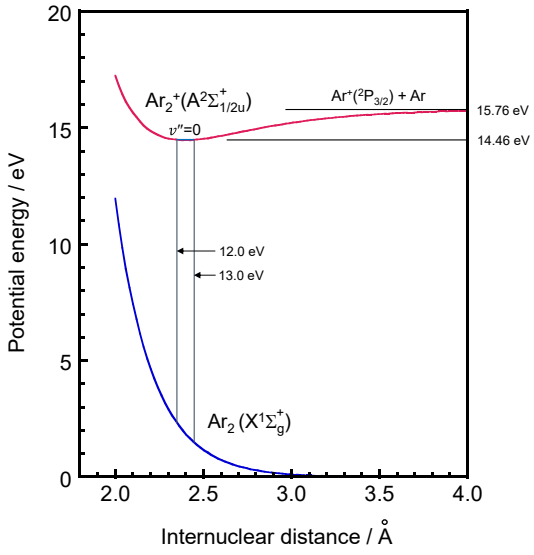

Fig. 6. Potential energy curves of $Ar_2^+(A^2\Sigma^+_{(1/2)u})$ and $Ar_2(X^1\Sigma^+_g)$. Morse potential of $Ar_2^+(A)$ was calculated by using molecular constants in Ref. 40, whereas the repulsive potential of $Ar_2(X)$ was calculated using a function reported in Ref. 41.

$Ar_2^+(A^2\Sigma^+_{(1/2)u}: v''=0)$ to be 12.6–13.5 eV[1] using reported molecular constants of $Ar_2^+(A^2\Sigma^+_{(1/2)u})$[43] and potential energy function of $Ar_2(X^1\Sigma_g^+)$.[41] In this study, the effective recombination energy of $Ar_2^+(A^2\Sigma^+_{(1/2)u}: v''=0)$ was re-evaluated to be 12.0–13.0 eV using more precise molecular constants of $Ar_2^+(A^2\Sigma^+_{(1/2)u})$.[40] The result obtained is shown in Fig. 6.

The ionization energy of $CS_2^+(\tilde{A}: v_1'=0)$ is 12.69 eV and those of $CS_2^+(\tilde{A}: v_1'=4,5)$ are 12.99 and 13.06 eV, respectively.[31] Thus, the $CS_2^+(\tilde{A}: v_1'>4)$ levels cannot be formed by the $Ar_2^+ + CS_2$ reaction energetically. In the $Ar_2^+ + CS_2$ reaction, low vibrational levels of $CS_2^+(\tilde{A})$ are preferentially formed and no continuous $CS_2^+(\tilde{A}\text{–}\tilde{X})$ emission can be observed. One reason for the absence of the continuous $CS_2^+(\tilde{A}\text{–}\tilde{X})$ emission is the endothermicity of the formation of high energy levels. The other reason is lower rotational excitation of $CS_2^+(\tilde{A})$.

4. Summary and Conclusion

We have previously observed $CS_2^+(\tilde{A}\text{–}\tilde{X})$ emission in an Ar flowing afterglow.[1] Although we attributed its excitation source to Ar_2^+, a later flow-tube study by Upshulte et al.[2] indicated that Ar^+ not Ar_2^+ is the responsible excitation source. Additional experiments in this flowing-afterglow study led us to conclude that our previous assignment of the excitation source is correct and strong discrete $CS_2^+(\tilde{A}\text{–}\tilde{X})$ emissions from low vibrationally excited states really arise from the $Ar_2^+ + CS_2$ reaction at high Ar pressures above ≈1 Torr. We separately studied the thermal-energy $Ar^+ + CS_2$ reaction using the He afterglow where the contribution from Ar_2^+ was excluded completely. Then, weak discrete $CS_2^+(\tilde{A}\text{–}\tilde{X})$ emissions from low vibrationally excited states were observed over strong continuous background emission, which was consistent with the previous observation of Upshulte et al.[2] The present results clearly show that both Ar^+ and Ar_2^+ ions can be excitation sources of $CS_2^+(\tilde{A}\text{–}\tilde{X})$ emission in the Ar afterglow with significantly different spectral features. The $Ar_2^+ + CS_2$ reaction was its dominant source at high Ar pressure above ≈1 Torr, whereas the $Ar^+ + CS_2$ reaction was responsible for the $CS_2^+(\tilde{A}\text{–}\tilde{X})$ emission at a low Ar pressure of 0.75 Torr. At intermediate pressure range of Ar, both Ar^+ and Ar_2^+ ions contributed to the $CS_2^+(\tilde{A}\text{–}\tilde{X})$ emission. Based on the present findings, both Ar^+ and Ar_2^+ ions were excitation sources of low-resolution $CS_2^+(\tilde{A}\text{–}\tilde{X})$ emissions obtained in the Ar flow-tube experiments by Upshulte et al.,[2] although the relative contribution of Ar^+ and Ar_2^+ ions depended on various experimental parameters they used.

Rincon et al.[5] reported that vibrational distribution of $CS_2^+(\tilde{A})$ in the thermal-energy $Ar^+ + CS_2$ reaction is essentially FC-like from the measurements of kinetic energy distribution of CS_2^+ using ICR spectrometer. However, the spectral features of the observed $CS_2^+(\tilde{A}\text{–}\tilde{X})$ emission from the $Ar^+ + CS_2$ reaction was completely different from those of VUV photoionization and Penning ionization, which proceed via vertical FC-like ionization. It was therefore concluded that the $Ar^+ + CS_2$ reaction takes place through non-FC-like ionization. The product ions were expected to be more vibrationally excited than those expected from FCFs for ionization. The formation of highly vibrationally and rotationally excited states with complicated band structures due to anharmonic and Fermi resonances and polyads interactions will be responsible for the appearance of strong continuous $CS_2^+(\tilde{A}\text{–}\tilde{X})$ emission. Re-examination of kinetic energy distribution of CS_2^+ obtained by Rincon et al. using ICR technique[5] suggested that internal (vibrational and rotational) energy distribution of $CS_2^+(\tilde{A})$ is more excited than FC-like vertical ionization. This result supported the formation of high rovibrationally excited states which provide strong continuous emission in the $Ar^+ + CS_2$ reaction.

Acknowledgments

This paper is dedicated to one of the co-authors Dr. Minoru Endoh who was working at Hitachi Metals, Ltd. and deceased in 2015.

References

1) M. Endoh, M. Tsuji, and Y. Nishimura, *Chem. Phys. Lett.*, 109, 35 (1984).
2) B. L. Upshulte, R. J. Shul, R. Passarella, R. E. Leuchtner, R. G. Keesee, and A. W. Castleman, Jr., *J. Phys. Chem.*, 90, 100 (1986).
3) H. Sekiya, M. Tsuji, and Y. Nishimura, *Chem. Phys. Lett.*, 100, 494 (1983).
4) K. Suzuki and K. Kuchitsu, *Bull. Chem. Soc. Jpn.*, 50, 1905 (1977).
5) M. E. Rincon, J. Pearson, and M. T. Bowers, *J. Phys. Chem.*, 92, 4290 (1988).
6) M. Endoh, PhD thesis, Graduate Schools of Eng. Sci., Kyushu Univ. (1984).
7) M. Tsuji, T. Funatsu, H. Kouno, Y. Nishimura, and H. Obase, *J. Chem. Phys.*, 96, 3649 (1992).
8) R. Johnsen, A. Chen, and M. A. Biondi, *J. Chem. Phys.*, 73, 1717 (1980).
9) F. W. Lee and C. B. Collins, *J. Chem. Phys.*, 65, 5189 (1976).

10) H. Hotop, A. Niehaus, and A. Schmeltekopf, *Z. Phys.*, 229, 1 (1969).
11) J. A. Herce, K. D. Foster, and E. E. Muschlitz, Jr., *Bull. Am. Phys. Soc.*, 13, 206 (1968).
12) W. P. West, T. B. Cook, F. B. Dunning, R. D. Rundel, and R. F. Stebbings, *J. Chem. Phys.*, 63, 1237 (1975).
13) C. E. Brion, C. A. McDowell, and W. B. Stewart, *J. Electron Spectrosc.*, 1, 113 (1972/73).
14) M. Tsuji, M. Furusawa, and Y. Nishimura, *Chem. Phys. Lett.*, 166, 363 (1990).
15) M. Tsuji, M. Furusawa, and Y. Nishimura, *J. Chem. Phys.*, 92, 6502 (1990).
16) N. G. Adams, D. K. Bohme, D. B. Dunkin, and F. C. Fehsenfeld, *J. Chem. Phys.*, 52, 1951 (1970).
17) I. Dabrowski, G. Herzberg, and K. Yoshino, *J. Mol. Spectrosc.*, 89, 491 (1981).
18) H. L. Kramer, J. A. Herce, and E. E. Muschlitz, Jr., *J. Chem. Phys.*, 56, 4166 (1972).
19) W. J. Balfour, *Can. J. Phys.*, 54, 1969 (1976).
20) M. Toyoda**,** T. Ogawa, and N. Ishibashi, *Bull. Chem. Soc. Jpn.*, 47, 95 (1974).
21) M. Tsuji, K. Mizukami, H. Sekiya, H. Obase, S. Shimada, and Y. Nishimura, *Chem. Phys. Lett.*, 107, 389 (1984).
22) A. J. Yencha and K. T. Wu, *Chem. Phys.*, 49, 127 (1980).
23) A. Benz, O. Leisin, H. Morgner, H. Seiberle, and J. Stegmaier, *Z. Phys. A*, 320, 11 (1985).
24) M. Tsuji and J. P. Maier, *Chem. Phys.*, 126, 435 (1988).
25) I. Tokue, T. Kudo, M. Kobayashi, and K. Yamasaki, *Bull. Chem. Soc. Jpn.*, 70, 71 (1997).
26) J. H. Callomon, *Proc. Roy. Soc. London A*, 244, 220 (1958).
27) G. Herzberg, "*Molecular Spectra and Molecular Structure III, Electronic Spectra and Electronic Structure of Polyatomic Molecules*", Krieger: Malabar, FL (1991).
28) D. C. Frost, S. T. Lee, and C. A. McDowell, *J. Chem. Phys.*, 59, 5484 (1973).
29) C. Y. Wu, T. S. Yih, and D. L. Judge, *Int. J. Mass Spectrom. Ion Process.*, 68, 303 (1986).
30) I. Tokue, H. Shimada, A. Masuda, Y. Ito, and H. Kume, *J. Chem. Phys.*, 93, 4812 (1990).
31) J. Liu, M. Hochlaf, G. Chambaud, P. Rosmus, and C. Y. Ng, *J. Phys. Chem. A*, 105*,* 2183 (2001).
32) C.-C. Zen and Y.-P. Lee, *Chem. Phys. Lett.*, 244, 177 (1995).
33) S.-G. He and D. J. Clouthiera, *J. Chem. Phys.*, 124, 084312 (2006).
34) H. Sekiya, M. Tsuji, and Y. Nishimura, *Chem. Phys. Lett.*, 100, 494 (1983).
35) M. Tsuji, J. P. Maier, H. Obase, H. Sekiya, and Y. Nishimura, *Chem. Phys. Lett.*, 137, 421 (1987).
36) G. Mauclaire, R. Derai, S. Fenistein, and R. Marx, *J. Chem. Phys.*, 70, 4017 (1979).
37) D. W. Turner, C. Baker, A. D. Baker, and C. R. Brundle, "*Molecular Photoelectron Spectroscopy* ", Wiley-Interscience, New York (1970).
38) D. C. Parent, R. Derai, G. Mauclaire, M. Heninger, R. Marx, M. E. Rincon, A. O'Keefe, and M. T. Bowers, *Chem. Phys. Lett.*, 117, 127 (1985).
39) R. J. Shul, R. Passarella, X. L. Yang, R. G. Keesee, and A. W. Castleman, Jr., *J. Chem. Phys.*, 87, 1630 (1987).
40) P. Rupper and F. Merkt, *J. Chem. Phys.*, 117, 4264 (2002).
41) L. Mattera, C. Salvo, S. Terreni, and F. Tommasini, *J. Chem. Phys.*, 72, 6815 (1980).
42) K.-M. Weitzel and J. Mähnert, *Int. J. Mass Spectrom.*, 214, 175 (2002).
43) P. A. Christiansen, K. S. Pitzer, Y. S. Lee, J. H. Yates, W. C. Ermler, and N. W. Winter, *J. Chem. Phys.*, 75, 5410 (1981).